XLVI CILAMCE
VITÓRIA - ES - BRAZIL - 2025
XLVI IBERO-LATIN AMERICAN CONGRESS ON COMPUTATIONAL METHODS IN ENGENEERING

Service life and reliability of reinforced concrete under chloride intrusion

Gustavo de M. S. Gidrão[1], Rúbia Mara Bosse[1], Henrique Kroetz[2], Laura Silvestro[1], Edson Denner Leonel[3]

[1]Programa de Pós-Graduação em Engenharia Civil, Universidade Tecnológica Federal do Paraná – UTFPR
gustavo.gidrao@utfpr.edu.br, rubia.bosse@utfpr.edu.br, laurasilvestro@utfpr.edu.br

[2]Universidade Federal do Paraná – UFPR
henrique.kroetz@ufpr.br

[3]Departamento de Engenharia de Estruturas, Escola de Engenharia de São Carlos – USP
edleonel@sc.usp.br

Abstract. This study presents the development and validation of a probabilistic computational framework for assessing the durability degradation of reinforced concrete structures subjected to chloride-induced corrosion. The methodology integrates Monte Carlo stochastic simulations with a finite volume discretization approach, implemented in Python using the FiPy library. This enables two-dimensional modeling of chloride ion diffusion through the concrete cover, accounting for time-dependent diffusion coefficients and boundary conditions calibrated from experimental and field data. The framework produces chloride concentration maps, structural reliability curves, and spatial distributions of failure probability. A graphical user interface (GUI) was developed to enhance usability and will be delivered as a registered intellectual product. Validation against experimental data from Xiong et al. (2022) demonstrated strong agreement in chloride profiles, confirming the precision of the proposed model. In addition, the framework was applied to compare different durability strategies, including silane-based surface protection and concrete based on LC3 with steel fibers. The results highlight the effectiveness of hydrophobic treatments in delaying the initiation of corrosion, while also revealing that concretes with alternative binders may require complementary protective measures. Furthermore, simulations demonstrated that the number of exposed surfaces significantly influences chloride ingress, reinforcing the importance of accurately defining boundary conditions in durability design.
Keywords: Monte Carlo simulations, chloride diffusion, durability, reinforced concrete, climate change.

1 Introduction

The durability of reinforced concrete elements is directly related to their electrical resistance to penetration of chloride ions, which is the main agent responsible for reinforcement corrosion. Assessment of structural vulnerability in the context of corrosion requires accurate predictive models that incorporate the combined effects of ion transport, corrosion kinetics, and degradation of the mechanical properties of materials [1, 2]. When the chloride concentration at the depth of the reinforcement reaches the critical threshold (generally 0.4% of the concrete mass), the depassivation phenomenon occurs, essentially characterized by a reduction in pH from around 14 to acidic values, triggering the corrosion process. This condition defines a serviceability limit state (SLS), as it marks the beginning of deterioration that compromises the durability of the structure, even if the structural integrity remains unaffected in the short term.

Once started, corrosion leads to expansive volumetric products that cause cracking and delamination of the concrete cover, as well as a reduction in the cross-sectional area of the steel reinforcement. These effects result in a loss of structural capacity, compromising the safety of the structure and violating the assumptions used in the structural design standards [3, 4].

Typically, chloride transport in porous concrete media is simplified using the one-dimensional (1D) transient diffusion equation derived from Fick's laws, which relates chloride flux to concentration gradient

and apparent diffusion coefficient [5], according to Eq. 1.

$$\frac{\partial C(x,t)}{\partial t} = D\frac{\partial^2 C(x,t)}{\partial x^2}, \tag{1}$$

Although the one-dimensional (1D) model is widely adopted due to its simplicity and low computational demand, it presents significant limitations when applied to real structural components. By assuming uniform material properties and boundary conditions throughout the section, it fails to represent multidirectional diffusion, localized degradation mechanisms, and geometric discontinuities such as corners, edges, or variations in concrete cover. Furthermore, the 1D approach cannot account for the combined effects of multiple exposed surfaces or the interaction between adjacent zones subjected to different environmental conditions. These simplifications reduce its predictive accuracy in nonuniform chloride ingress scenarios, particularly in elements with complex geometries or when spatial variability is critical for reliability analysis and failure probability estimation.

To address this, the present study adopts a two-dimensional (2D) formulation based on Fick's second law, which combines mass conservation with Fick's first law [6], as described in Equations 2–7:

$$\mathbf{J} = -D(t)\,\nabla C, \tag{2}$$

$$\frac{\partial C}{\partial t} = \nabla \cdot (D(t)\nabla C) \tag{3}$$

where:

$$D(t) = D_{\text{ref}} \left(\frac{T_{\text{ref}}}{T_{\text{ref}} + t} \right)^m, \tag{4}$$

$$T_{\text{ref}} = T_{\text{ref}_{\text{years}}} \times 365.25 \times 24 \times 3600, \tag{5}$$

with time expressed in seconds.

The Dirichlet boundary condition at the active surface is given by:

$$C\big|\partial\Omega(t) = C_s(t) = Cs0 + k\sqrt{\frac{t}{T_{\text{ref}}}}, \tag{6}$$

and the initial condition is:

$$C(x, y, 0) = 0. \tag{7}$$

Given the context mentioned above, it is possible to postulate that the serviceability limit state (SLS) is reached when the chloride concentration at the steel–concrete interface exceeds a critical threshold, typically around 0.4% [7], triggering corrosion initiation. This condition does not represent immediate structural collapse, but compromises the durability and functionality of the structure. Upon reaching the critical chloride level of 0.4% at the steel–concrete interface [7], pitting corrosion begins, leading to cracking and cross-sectional reduction, thus diminishing the flexural and shear capacities of steel bars [8]. Although structural failure is not immediate, this poses an issue for serviceability.

Hence, the corresponding limit state function for each realization i at time t_k is expressed as:

$$g_i(t_k) = \bar{C}_{\text{th},i} - C_i(x, y_{\text{reb}}, t_k), \tag{8}$$

where $C_i(x, y_{\text{reb}}, t_k)$ is the chloride concentration at the reinforcement depth, and $\bar{C}_{\text{th},i}$ is the critical threshold concentration that initiates corrosion. The SLS is violated when $g_i(t_k) < 0$.

The simplest measure to prevent this pathological process is to ensure appropriate reinforcement cover in accordance with the exposure classes in design codes, along with quality control during construction [9]. Alternatively, to mitigate chloride-induced corrosion in reinforced concrete, methods such as decreasing concrete permeability can be employed. Notable techniques include the use of ultra-high-performance concrete (UHPC) [10, 11, 12, 13], the integration of additional cementitious materials such as silica fume and metakaolin [14], the application of particle packing techniques [15, 16], the use of protective coatings such as silane and siloxane [7], and the use of corrosion inhibitors to slow reinforcement corrosion [17]. These methods focus on reducing the diffusion coefficient of concrete.

To address these challenges, this study develops and applies a two-dimensional numerical framework to simulate chloride diffusion in reinforced concrete elements, incorporating time-dependent parameters

and probabilistic input distributions. Initially, a deterministic model is validated against experimental data from Xiong et al.[18] and numerical results obtained through a three-dimensional simulation in Abaqus, demonstrating its precision in reproducing chloride penetration profiles. Subsequently, the analysis is extended to a real-scale reinforced concrete beam made of normal-strength concrete, subjected to chloride ingress from two exposed faces. The reference case is then compared to a similar beam treated with silane-based surface protection, allowing for the evaluation of its effectiveness in improving durability. Finally, scenarios with chloride exposure on two and four faces are compared to assess the influence of surface exposure conditions on structural reliability and probability of failure over time.

2 Computational Model and Probabilistic Assessment

This section presents the numerical framework and code developed to simulate chloride entry and estimate the probability of reinforcement depassivation in reinforced concrete structures. The algorithm was fully implemented in Python, and a standalone executable was generated to facilitate its use without requiring additional dependencies or coding expertise. The tool was designed to be flexible, enabling its application to various types of concrete, exposure conditions, and ages, making it suitable for both academic research and engineering practice.

The simulations employ the FiPy library for discretization of finite volumes. Uncertainties are treated using a Monte Carlo approach. The input parameters are modeled using log-normal, normal, or uniform distributions, depending on the physical characteristics of each variable and the availability of experimental or normative data. Initially, probabilistic distributions are defined for the reference diffusivity D_{ref}, initial surface concentration C_{s0}, reinforcement cover depth, and the critical chloride threshold $\bar{C}_{\text{th},i}$, as well as the number of Monte Carlo realizations N. Mean values and standard deviations can be obtained from experimental studies [19, 7, 18] or specialized guidelines such as the Joint Committee on Structural Safety [20].

A regular mesh (Grid2D) is generated to represent the cross section of the structural member, and the coordinates of the monitored reinforcement positions are defined. For each realization $i = 1, \ldots, N$, independent samples of the input parameters are drawn and a time loop is executed from $t = 0$ to the maximum service life. At each discrete time step t_k, the effective diffusion coefficient is updated according to:

$$D(t_k) \;=\; D_{\text{ref},i} \left(\frac{T_{\text{ref}}}{T_{\text{ref}} + t_k} \right)^m, \tag{9}$$

and the surface concentration evolves following:

$$C_s(t_k) \;=\; C_{s0,i} + k \sqrt{\frac{t_k}{T_{\text{ref}}}}, \tag{10}$$

as described by Xiong et al. [18]. Boundary conditions are applied, and the weak form of the diffusion equation is solved using the implicit Backward–Euler scheme. At each time step, the chloride concentration field $C_i(x, y, t_k)$ is updated, and concentrations at the reinforcement positions are recorded.

After completing the time and Monte Carlo loops, a post-processing stage is performed. The average spatial chloride concentration is computed as:

$$\overline{C}(x, y) \;=\; \frac{1}{N} \sum_{i=1}^{N} C_i(x, y), \tag{11}$$

The time-dependent probability of failure is estimated based on the exceedance of the critical threshold:

$$P_{\text{f}}(t_k) \;=\; \frac{1}{N} \sum_{i=1}^{N} \mathbf{H}\big\{ C_i(x, y_{\text{reb}}, t_k) > \bar{C}_{\text{th},i} \big\}, \tag{12}$$

where $\mathbf{H}$ is the Heaviside indicator function, equal to 1 if the condition is met (failure) and 0 otherwise. In addition, a two-dimensional failure probability map is generated to visualize the spatial distribution of corrosion risk across the cross section.

Preliminary tests show that the simulation runs in approximately one minute per realization using a 1,000-element mesh, enabling structural reliability projections over a 100-year time horizon. The general

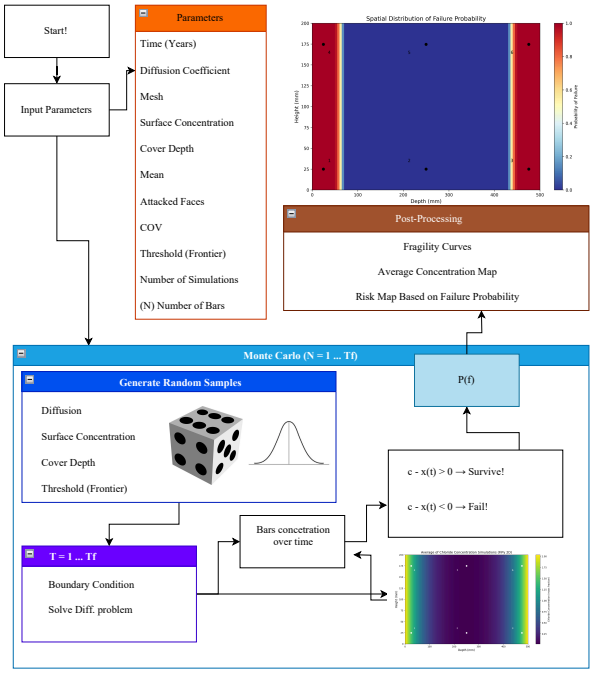


Figure 1. Flowchart of the stochastic simulation algorithm for chloride diffusion.

structure of the proposed computational framework, including the sampling of input parameters, the numerical solution loop, and the post-processing routines, is summarized in the flow chart presented in Figure 1. This diagram illustrates the step-by-step sequence of the stochastic simulation algorithm used to model chloride diffusion and estimate failure probabilities in reinforced concrete structures. The computational framework, including the sampling of input parameters, the numerical solution loop, and the post-processing routines, is summarized in the flow chart presented in Figure 1.

3 Deterministic Validation

To demonstrate technical feasibility and validate the code developed, a numerical experimental simulation based on the study by Xiong et al. [18] is proposed. In this work, the authors calibrated chloride diffusion models in concrete considering the temporal variability of both the diffusion coefficient and the surface concentration, showing a significantly better correlation with experimental profiles compared to classical 1D models. Figure 2 compares the experimental data obtained after four years [18] with the numerical results of the developed model (FiPy2D), as well as a 3D simulation performed in Abaqus, which simulates diffusion on one surface of a concrete prism, in therms of percentual error (Fig. 2 .a) and absolute concentration in the profile of the beam (Fig. 2 .b).To validate the developed code and demonstrate its technical feasibility, a numerical simulation was carried out based on the experimental study by Xiong et al. [18]. In that work, the authors calibrated chloride diffusion models in concrete taking into account the time-dependent behavior of both the diffusion coefficient and the surface concentration, achieving significantly improved agreement with experimental profiles when compared to classical 1D formulations.

Figure 2 presents a comparative analysis between the experimental results obtained after four years of exposure and the numerical predictions of the 2D FiPy model, as well as a 3D simulation performed in Abaqus, which simulates chloride ingress through a single exposed surface of a concrete prism. Figure 2a.a illustrates the relative error between the experimental and simulated results, while the figure 2b.b compares the absolute chloride concentration profiles along the depth of the concrete section. Table 1 presents the model‘s parameters.

The numerical profiles obtained with both the FiPy 2D model and the Abaqus 3D simulation accurately reproduce the exponential decay trend observed in the experimental chloride concentration after four years of exposure. For depths greater than 30 mm, both models align almost perfectly and fall within the experimental dispersion range, indicating that the code developed and the Abaqus implementation are equally capable of capturing deep diffusion behavior.

Table 1. Main parameters of the numerical model [18]

Parameter	Symbol	Value
Reference diffusivity	D_{ref}	$3.78 \times 10^{-6}\,\text{mm}^2/\text{s}$ ($3.78 \times 10^{-12}\,\text{m}^2/\text{s}$)
Reference time	T_{ref}	1.00 year (3.156×10^7 s)
Aging exponent	m	0.23
Total exposure time	T_{total}	4.00 years (1.262×10^8 s)
Section dimensions	L_x, L_y	50.27 mm, 30.00 mm
Numerical mesh	n_x, n_y	20, 20
Time step	Δt	2.63×10^6 s
Number of steps	—	48
Initial surface concentration	C_{s0}	0.01
Build-up coefficient	k	0.21

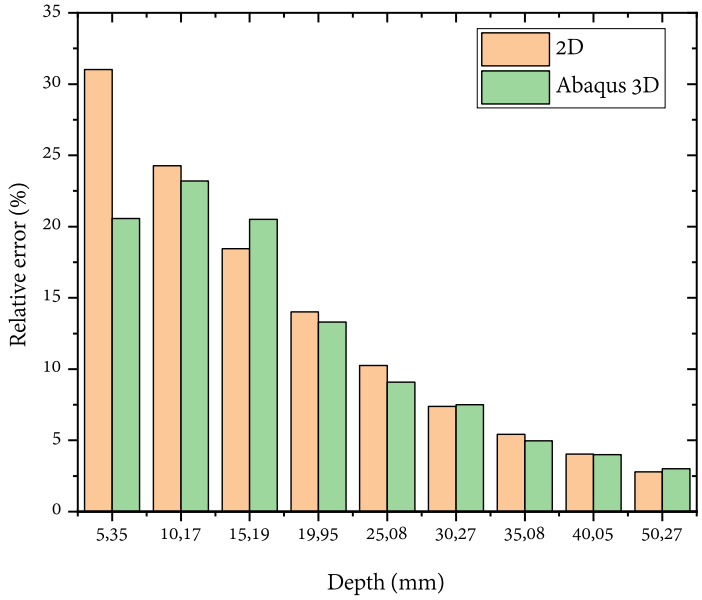
However, in the shallower region (up to approximately 15 mm), Abaqus tends to slightly overestimate concentrations, while FiPy presents a slight underestimation. These differences may arise from the implementation of the boundary condition, especially the surface concentration evolution model, or from the level of mesh refinement and diffusivity parameters used in each solver. Notably, Abaqus uses second-order integration elements, which may increase chloride retention near the boundary, while FiPy, using a structured mesh, results in a slightly faster internal diffusion response.

In summary, both computational models provide reliable predictions, with relative errors typically below 10% for depths beyond 20 mm, and successfully capture the observed dispersion profile. For further refinement, it is recommended to locally calibrate the diffusion coefficient and $C_s(t)$ evolution from field data, and to explore adaptive mesh refinement and coupling with chloride binding reactions. Thus, the numerical model can become even more robust for the estimation of the service life and the design of the durability of reinforced concrete structures.

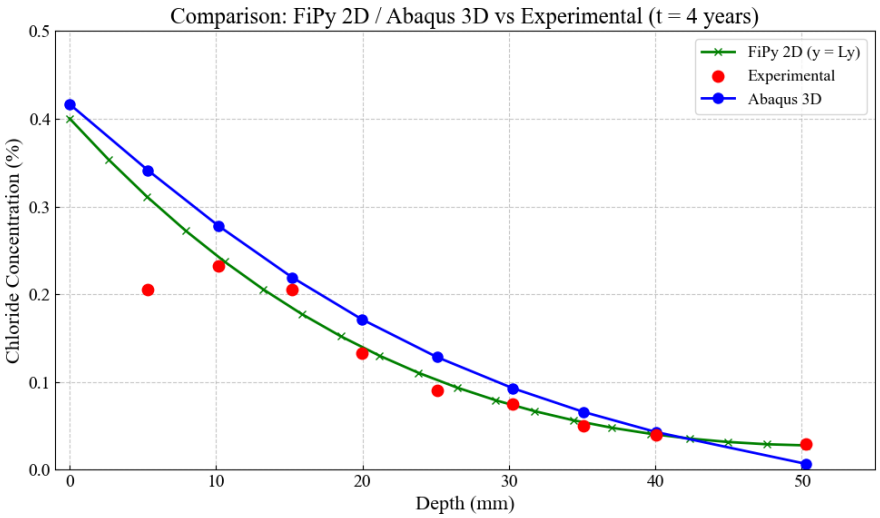
It is worth highlighting that the FiPy 2D model and the Abaqus 3D simulation show close agreement in terms of chloride penetration profiles, particularly for depths exceeding 30 mm, validating both against four-year experimental results. However, while the 2D FiPy model offers faster computation times and is suitable for Monte Carlo simulations, the 3D Abaqus model enables higher fidelity by capturing longitudinal variations and material or geometric heterogeneities.

The relative error between the numerical predictions and the experimental chloride concentrations is shown in Figure 2.b. As expected, the 3D Abaqus model provides better agreement with the experimental data, particularly near the exposed surface, where the 2D FiPy model tends to overestimate chloride penetration. This discrepancy, while relevant for deterministic assessments, becomes less critical at greater depths, where both models converge to errors below 10 %. Despite its limitations, the 2D model demonstrated acceptable accuracy within the range of interest for structural performance evaluation. More importantly, its significantly lower computational cost makes it suitable for large-scale probabilistic analyses. For this reason, the 2D model was adopted for the Monte Carlo simulations, allowing the propagation of input uncertainties through thousands of realizations without compromising computational efficiency.

In terms of computational efficiency, the Abaqus 3D simulation required approximately 50 seconds to complete the analysis, whereas the FiPy 2D model executed the same scenario in just 4 seconds. This substantial difference in runtime reinforces the practical viability of the 2D approach for large-scale reliability assessments and probabilistic durability analyses, where thousands of simulations are often needed. The low computational cost of the FiPy model, combined with its ability to capture the essential trends of chloride penetration, makes it a valuable tool for Monte Carlo frameworks and service life prediction in engineering practice.



(a) Relative error (%) between 2D FiPy and experimental data.



(b) Comparison between 3D Abaqus and experimental data.

Figure 2. Relative error (%) between the numerical models and experimental data as a function of depth.

Table 2. Stochastic input parameters used in the probabilistic simulation ($N = 1000$).

Parameter	Description	Mean Value	COV
D_{ref}	Reference diffusivity ($\times 10^{-12}$ m^2/s)	3.78	0.10
C_{s0}	Initial surface chloride content (fraction)	0.01	0.10
Cover	Concrete cover (mm)	25	0.10
Threshold	Corrosion initiation threshold (fraction)	0.40	0.10

4 Probabilistic Assesment

The input parameters adopted in the probabilistic simulations are summarized in Table 2. These include stochastic variables related to the diffusion process, material properties, and geometric configuration of the concrete beam. A Monte Carlo approach with realizations of $N = 1000$ was employed to propagate the uncertainties.

In addition, a comparative scenario was analyzed considering the application of a silane-based surface treatment. In this case, the diffusion coefficient D_{ref} was reduced by 69%, as reported in the literature for effective hydrophobic treatments. All other parameters were kept unchanged, allowing a direct evaluation of the impact of treatment on chloride ingress and corrosion risk.

5 Reliability analysis

In this example, the developed probabilistic framework was applied to assess the durability performance of various concrete materials exposed to chloride ingress. Several concretes with different diffusion coefficients were analyzed, including reference concrete (NSC), silane-treated surface samples, and an alternative binder based on limestone calcinated clay cement (LC3) reinforced with steel fibers [21].

The analysis accounted for variations in the diffusion coefficient, the number of exposed faces, and protective treatments, with the aim of predicting the time-dependent probability of reaching the corrosion initiation threshold. Additionally, a scenario simulating chloride ingress on four faces was modeled for the NSC, allowing comparison with the standard two-face exposure condition. Table 3 presents the developed examples.

Table 3. Analyzed scenarios in the probabilistic durability assessment

Concrete Type	Silane Treatment	No. of Exposed Faces	Reference
NSC (Reference)	No	2 Faces	Validated [18]
NSC (4 Faces)	No	4 Faces	Validated [Xiong]
NSC + Silane	Yes	2 Faces	[22]
LC3 + Steel Fibers	No	2 Faces	[21]

Figure 3 shows the comparison among the above-mentioned mixtures. By reducing the reference diffusion coefficient (D_{ref}) by 69% [22], silane significantly delays chloride ingress over time and, therefore, reduces the probability of reaching the corrosion initiation threshold within the service life, emphasizing the potential of hydrophobic treatments as a practical strategy to extend the durability of concrete structures exposed to aggressive environments.

In contrast, the LC3-based mixture with 2% steel fibers, although an alternative binder with reduced clinker content and promising mechanical behavior, exhibits a higher probability of corrosion initiation compared to silane-treated concrete. This suggests that, although LC3 represents a sustainable alternative, additional protective measures may be required to improve its durability under chloride exposure. Furthermore, the scenario that simulates chloride ingress on all four faces of the NSC highlights the critical role of exposure conditions. The increase in exposed surfaces significantly accelerates the deterioration process, reinforcing the importance of accurately defining boundary conditions in durability design. This underscores the ability of the proposed probabilistic model to assess various real-world exposure scenarios and support performance-based durability design.

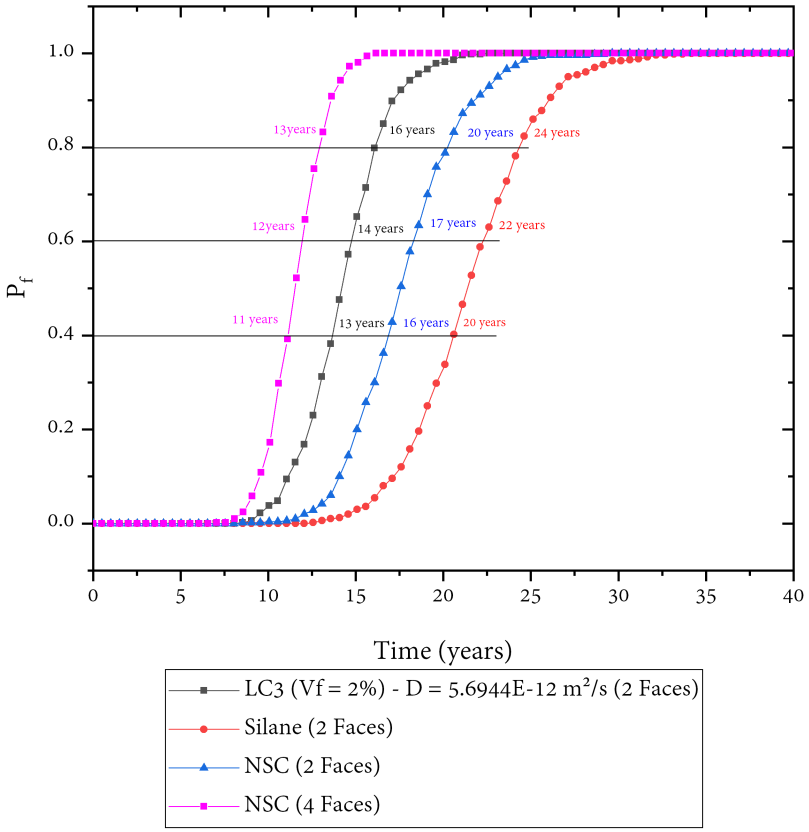


Figure 3. Failure probability

6 Conclusions

This study proposed and validated a two-dimensional probabilistic computational framework to evaluate the service life and reliability of reinforced concrete structures subjected to chloride-induced corrosion. By incorporating time-dependent diffusion parameters, spatially variable boundary conditions, and the modeling of multiple exposed surfaces, the framework enables more realistic simulations than traditional 1D approaches.

Validation against experimental data and 3D numerical simulations confirmed the precision of the proposed 2D model, especially at intermediate and deeper regions, while maintaining high computational efficiency, a key advantage for large-scale Monte Carlo simulations in performance-based design.

The probabilistic assessment compared different material and protection strategies. Normal Strength Concrete (NSC) treated with silane exhibited significantly improved durability, with a substantial reduction in the probability of reaching the corrosion initiation threshold. In contrast, LC3-based concrete with 2% steel fibers, despite its sustainable advantages and promising mechanical behavior, showed higher probabilities of initiation of corrosion under the same exposure conditions. This suggests the potential need to combine LC3 with protective measures such as silane to enhance its performance in aggressive environments.

Furthermore, the analysis highlighted the critical influence of exposure conditions, particularly the number of exposed surfaces. The simulation of chloride ingress through four faces resulted in a noticeably shorter service life, emphasizing the importance of accurately defining boundary conditions in durability design. These findings demonstrate the relevance and adaptability of the proposed model for evaluating different concretes and exposure scenarios, supporting performance-based decisions in structural durability design.

Bibliography

[1] Runqing Yu et al. “Life cycle embodied energy analysis of RC structures considering chloride-induced corrosion in seismic regions”. In: Structures 25 (Apr. 2020), pp. 839–848. ISSN: 2352-0124. DOI: 10.1016/j.istruc.2020.03.049. URL: https://doi.org/10.1016/j.istruc.2020.03.049.

[2] Jin Xia et al. Corrosion prediction models for steel bars in chloride-contaminated concrete: a review. July 2020. DOI: 10.1680/jmacr.20.00106. URL: https://doi.org/10.1680/jmacr.20.00106.

[3] Giovanni Pellizzer et al. “Reinforced concrete time-dependent reliability considering penetration of chlorides via boundary element method”. In: Latin American Journal of Solids and Structures 17 (Jan. 2020). DOI: 10.26678/abcm.mecsol2019.msl19-0069. URL: https://doi.org/10.26678/abcm.mecsol2019.msl19-0069.

[4] Fu Yuan Chong, Ya Nan An, and Peng Wang. “Research on Factors Affecting Reinforced Concrete Durability”. In: Advanced materials research 898 (Feb. 2014), pp. 403–406. ISSN: 1022-6680, 1662-8985. DOI: 10.4028/www.scientific.net/amr.898.403. URL: https://doi.org/10.4028/www.scientific.net/amr.898.403.

[5] Sakdirat Kaewunruen et al. “Vulnerability of Structural Concrete to Extreme Climate Variances”. In: Climate 6 (2 May 2018), pp. 40–40. ISSN: 2225-1154. DOI: 10.3390/cli6020040. URL: https://doi.org/10.3390/cli6020040.

[6] Caio Gorla Nogueira, Edson Denner Leonel, and Humberto Breves Coda. “Probabilistic failure modelling of reinforced concrete structures subjected to chloride penetration”. In: International Journal of Advanced Structural Engineering 4 (1 Dec. 2012). ISSN: 20086695. DOI: 10.1186/2008-6695-4-10.

[7] Rúbia Mara Bosse et al. “Reliability and Durability Assessment of Recycled Aggregate Concrete under Chloride Ingress: Design Optimization and Service Life Implications”. In: Case Studies in Construction Materials 21 (Dec. 2024). ISSN: 2214-5095. DOI: 10.1016/j.cscm.2024.e04045. URL: https://doi.org/10.1016/j.cscm.2024.e04045.

[8] Amit Kenny and Ela Ofer Rozovsky. “Six-Year-Old Ecological Concrete in a Marine Environment: A Case Study”. In: Sustainability 15 (18 Sept. 2023), pp. 13780–13780. ISSN: 2071-1050. DOI: 10.3390/su151813780. URL: https://doi.org/10.3390/su151813780.

[9] F. Bolzoni et al. “Progresses in prevention of corrosion in concrete”. In: vol. 296. IOP Publishing, July 2019, pp. 12016–12016. DOI: 10.1088/1755-1315/296/1/012016. URL: https://doi.org/10.1088/1755-1315/296/1/012016.

[10] Cheng Chen, Haiyang Cai, and Lijuan Cheng. “Shear strengthening of corroded RC beams using UHPC–FRP composites”. In: Journal of Bridge Engineering 26 (1 Jan. 2021), p. 4020111. ISSN: 1084-0702. DOI: 10.1061/(asce)be.1943-5592.0001653. URL: https://doi.org/10.1061/(asce)be.1943-5592.0001653.

[11] Ben Graybeal. “Design and construction of field-cast UHPC connections”. In: FHWA-HRT-08-044 (Oct. 2014). URL: https://rosap.ntl.bts.gov/view/dot/28283.

[12] R. D. Toledo Filho et al. “Performance assessment of ultra high performance fiber reinforced cementitious composites in view of sustainability”. In: Materials and Design 36 (Jan. 2012), pp. 880–888. ISSN: 02641275. DOI: 10.1016/j.matdes.2011.09.022. URL: http://dx.doi.org/10.1016/j.matdes.2011.09.022.

[13] Graybeal and Tanesi. “Durability of an ultrahigh-performance concrete”. In: JOURNAL OF MATERIALS IN CIVIL ENGINEERING 19 (10 Jan. 2007), pp. 848–854. ISSN: 08991561. DOI: 10.1061/HÇASCEHŸ0899-1561HÇ2007HŸ19:10HÇ848HŸ. URL: https://doi.org/10.1061/(asce)0899-1561(2007)19:10(848).

[14] Rahat Ullah et al. Ultra-High-Performance Concrete (UHPC): A State-of-the-Art Review. June 2022. DOI: 10.3390/ma15124131. URL: https://doi.org/10.3390/ma15124131.

[15] F. de Larrard and T. Sedran. “Optimization of ultra-high-performance concrete by the use of a packing model”. In: Cement and Concrete Research 24 (6 Jan. 1994), pp. 997–1009. DOI: 10.1016/0008-8846(94)90022-1. URL: https://doi.org/10.1016/0008-8846(94)90022-1.

[16] Olivier Bonneau et al. “Characterization of the granular packing and percolation threshold of reactive powder concrete”. In: Cement and Concrete Research 30 (12 Jan. 2000), pp. 1861–1867. ISSN: 00088846. DOI: 10.1016/S0008-8846(00)00300-8. URL: https://doi.org/10.1016/s0008-8846(00)00300-8.

[17] L. Yohai, M. Vázquez, and M.B. Valcarce. “Phosphate ions as corrosion inhibitors for reinforcement steel in chloride-rich environments”. In: Electrochimica Acta 102 (Apr. 2013), pp. 88–96. ISSN: 0013-4686, 1873-3859. DOI: 10.1016/j.electacta.2013.03.180. URL: https://doi.org/10.1016/j.electacta.2013.03.180.

[18] Qing Xiang Xiong et al. “Chloride Diffusion Prediction in Concrete through Mathematical Models Based on Time–Dependent Diffusion Coefficient and Surface Chloride Concentration”. In: Journal of Materials in Civil Engineering 34 (11 Nov. 2022). ISSN: 0899-1561. DOI: 10.1061/(asce)mt.1943-5533.0004429.

[19] Gabriela Nunes Malysz et al. “Service-life prediction of recycled coarse aggregate concrete under natural carbonation: A time-dependent reliability analysis”. In: Construction and Building Materials 387 (July 2023). ISSN: 09500618. DOI: 10.1016/j.conbuildmat.2023.131632.

[20] Joint Committee on Structural Safety (JCSS). JCSS Probabilistic Model Code. Available from https://www.jcss-lc.org. Joint Committee on Structural Safety. 2010. ISBN: 978-3-909386-79-6.

[21] Laura Silvestro et al. “Rheological behavior, hydration, and mechanical properties of LC 3 systems with the incorporation of functionalized multi-walled carbon nanotubes”. In: Rev. IBRACON Estrut. Mater 17 (1 2024), p. 2024. DOI: 10.48331/scielodata.YB6XVR. URL: https://doi.org/10.48331/scielodata.YB6XVR..

[22] Rúbia Mara Bosse et al. “Reliability and durability assessment of recycled aggregate concrete under chloride ingress: Design optimization and service life implications”. In: Case Studies in Construction Materials 21 (Dec. 2024), e04045. ISSN: 2214-5095. DOI: 10.1016/j.cscm.2024.e04045. URL: http://dx.doi.org/10.1016/j.cscm.2024.e04045.